

## Article

# Petrographic and Chemical Characterization of the Frescoes by Saturnino Gatti (Central Italy, 15th Century)

Luigi Germinario <sup>1</sup>, Lorena C. Giannossa <sup>2,3</sup>, Marco Lezzerini <sup>4</sup>, Annarosa Mangone <sup>2,3</sup>, Claudio Mazzoli <sup>1</sup>, Stefano Pagnotta <sup>4</sup>, Marcello Spampinato <sup>4</sup>, Alfonso Zoleo <sup>5</sup> and Giacomo Eramo <sup>3,6,\*</sup>

<sup>1</sup> Department of Geosciences, University of Padua, 35131 Padova, Italy; luigi.germinario@gmail.com (L.G.); claudio.mazzoli@unipd.it (C.M.)

<sup>2</sup> Department of Chemistry, University of Bari Aldo Moro, 70125 Bari, Italy; lorenacarla.giannossa@uniba.it (L.C.G.); annarosa.mangone@uniba.it (A.M.)

<sup>3</sup> Interdepartmental Center Research Laboratory for the Diagnostics of Cultural Heritage, University of Bari Aldo Moro, 70125 Bari, Italy

<sup>4</sup> Department of Earth Sciences, University of Pisa, 56126 Pisa, Italy; marco.lezzerini@unipi.it (M.L.); stefano.pagnotta@unipi.it (S.P.); marcello.spampinato@unipi.it (M.S.)

<sup>5</sup> Department of Chemical Sciences, University of Padua, 35131 Padova, Italy; alfonso.zoleo@unipd.it

<sup>6</sup> Department of Geoenvironmental and Earth Sciences, University of Bari Aldo Moro, 70125 Bari, Italy

\* Correspondence: giacomo.eram@uniba.it

**Abstract:** This study presents the petrographic and chemical characterization of the frescoes in the Church of San Panfilo in Tornimparte (AQ, Italy) by Saturnino Gatti, a prominent painter of the late 15th–early 16th century, known for his exquisite technique, composition, and use of color. The characterization of the frescoes is essential for understanding the materials and techniques used by Gatti, as well as for identifying the stratigraphy and painting phases. Eighteen samples were collected from the original paint layers, later additions (17th century), and restored surfaces, and analyzed by optical microscopy, cathodoluminescence microscopy, scanning electron microscopy (SEM-EDS),  $\mu$ -Raman, and electron paramagnetic resonance (EPR). The analyses revealed a microstratigraphy often made of three main layers: (1) preparation, consisting of lime plaster and sand; (2) pigmented lime, applied by the fresco technique; and (3) additional pigmented layer on the surface. The most often recurring pigments are black, red, yellow (all generally linked with the fresco technique), and blue (applied “a secco”). The presence of two painting phases was also noted in one sample, probably resulting from a rethinking or restoration. These findings contribute to the understanding of the history and past restoration works of this cultural heritage site, providing important insights not only for conservators and restorers, but also for a broader understanding of Italian fresco painting and art history of the late 15th and early 16th centuries.

**Keywords:** lime plaster; fresco painting; pigments; paint stratigraphy; mineralogy; petrography; SEM-EDS; Raman; EPR; Tornimparte



**Citation:** Germinario, L.; Giannossa, L.C.; Lezzerini, M.; Mangone, A.; Mazzoli, C.; Pagnotta, S.; Spampinato, M.; Zoleo, A.; Eramo, G. Petrographic and Chemical Characterization of the Frescoes by Saturnino Gatti (Central Italy, 15th Century). *Appl. Sci.* **2023**, *13*, 7223. <https://doi.org/10.3390/app13127223>

Academic Editors: Juan García Rodríguez and Vittoria Guglielmi

Received: 15 April 2023

Revised: 12 May 2023

Accepted: 13 June 2023

Published: 16 June 2023



**Copyright:** © 2023 by the authors. Licensee MDPI, Basel, Switzerland. This article is an open access article distributed under the terms and conditions of the Creative Commons Attribution (CC BY) license (<https://creativecommons.org/licenses/by/4.0/>).

## 1. Introduction

The Italian painter Saturnino Gatti was known for his exceptional technique, composition, and use of color in his frescoes during the late 15th and early 16th centuries [1]. The Church of San Panfilo in Villagrande di Tornimparte (AQ, central Italy) is home to a significant example of his work, which is of considerable importance in the context of Italian cultural heritage [2]. The church is located in an area hit by the catastrophic earthquake of L’Aquila in 2009, but did not suffer any serious damage, contrary to many other buildings of historical and cultural significance. Studying the building, along with the artworks contained in it, will aid in its conservation and restoration [3,4].

Thanks to modern technologies, the characterization and reconstruction of altered or damaged painted surfaces can be achieved in various ways, ranging from techniques

for the restitution of morphology and color [5,6] to mineralogical–petrographic and chemical characterization techniques [7–9], frequently with non-destructive [10,11] and non-invasive [12–18] methodologies.

The study of the pictorial cycle in the Church of San Panfilo was conducted through a petrographic, mineralogical, and chemical approach. The investigation aimed to identify the stratigraphy, microstructure, and composition of the plasters [19], paint layers [20], and painting techniques [7,21,22]. The study also explored the presence of compounds possibly related to the alteration processes of the frescoes and their components [23]. The analyses may provide useful indications for a comprehensive understanding of the artistic technique of Saturnino Gatti and the conservation of the frescoes. The upcoming restoration of the church will be based on the principles of reversibility, compatibility, and durability. In this context, a multi-analytical approach, as demonstrated by Bersani et al. [24], Romani et al. [25], and Alberghina et al. [26], is extremely effective in providing information, from the macro to the micro domain [27], not only on pigments but also on specific binders (such as egg whites, oils, and resins) and alteration patinas [28]. The combination of this information can guide the restorer in the decision and implementation of specifically targeted conservation practices, useful for restoring the condition and readability of the artwork in case of ordinary and extraordinary maintenance [29–31], even with bioremediation techniques [32].

This paper is part of the Special Issue “Results of the II National Research Project of AIAr: archaeometric study of the frescoes by Saturnino Gatti and workshop at the Church of San Panfilo in Tornimparte (AQ, Italy)” [33], which presents the scientific results of the II National Research Project conducted by members of the Italian Association of Archaeometry (AIAr). The aim of the project was to conduct an in-depth study of the frescoes by Saturnino Gatti and his workshop, with the objective of contributing to a broader understanding of Italian fresco painting and art history of the late 15th and early 16th centuries. For a more detailed overview of the project’s objectives, the readers can refer to the introduction of the Special Issue [33].

## 2. Materials and Methods

### 2.1. Sampling

The sampling campaign was carried out on 1 March 2021, under the supervision of the officials of Soprintendenza Archeologia, Belle Arti e Paesaggio for the provinces of L’Aquila and Teramo. A total of 18 out of 47 samples collected from the paint layers and plasters of the frescoes were analyzed by this research group. Table 1 shows their original location and brief description. Some consist of multiple specimens; in that case, the alphanumeric ID is associated with a letter with alphabetical progression. The sampling areas considered here are the following (Figure 1): Panel A (The Kiss of Judas and the Capture of Christ); Panel B (Flagellation and Crowning with Thorns/Christ at the Column—a depiction that was extensively reworked, probably during the 17th century); Panel C (central wall of the apse with a window opened in 1926; originally, the Crucifixion was depicted there, a fragment of which still remains); Panel D (Lamentation over the Dead Christ); Panel E (Resurrection); and Vault (God the Father in Glory among angels and saints).

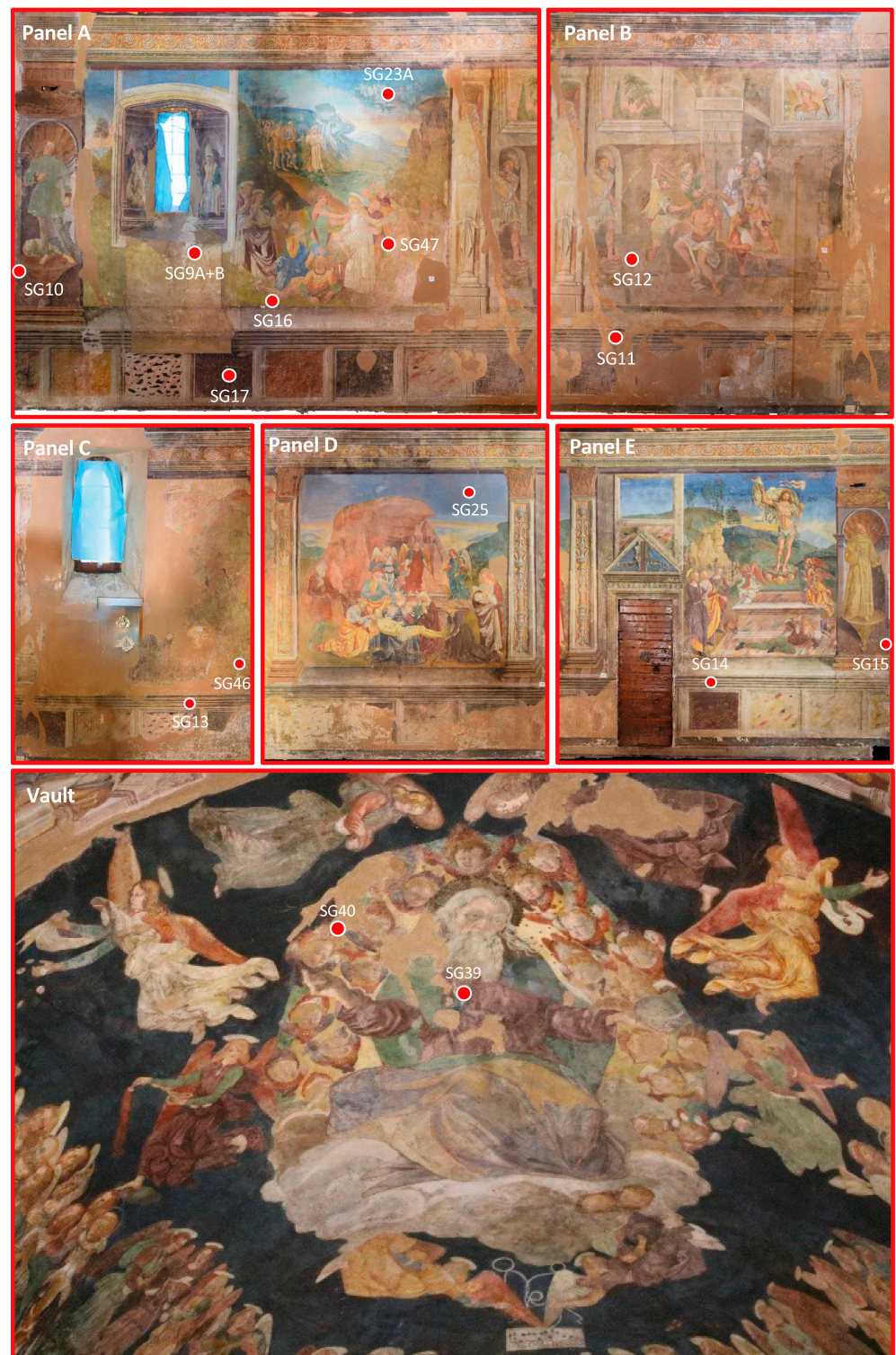


Figure 1. Sampling spots with associated sample ID.

**Table 1.** Source and macroscopic features of the analyzed samples (the question marks indicate doubtful interpretations requiring in-depth validation). The analytical techniques applied for each sample (“t.s.” = thin section; “f.” = fragment with no prior preparation) are also specified (details follow in Section 2.2).

Sample	Panel	Description	Investigation Technique
SG9A	A	Plaster with pale ochre paint	OM, SEM-EDS (t.s.)
SG9B	A	Plaster with pale ochre paint and decay products (?)	OM, SEM-EDS (t.s.)
SG10	A	Plaster with violaceous paint	OM, SEM-EDS (t.s.)
SG11	B	Plaster with dark-brown paint	OM, SEM-EDS (t.s.)
SG12	B	Plaster with blue–gray paint and makeover (?)	OM, SEM-EDS (t.s.)
SG13	C	Plaster with white paint	OM, SEM-EDS (t.s.)
SG14	E	Plaster with dark paint and protective coating (?)	OM, SEM-EDS (t.s.)
SG15	E	Plaster with blue layer	OM, SEM-EDS (t.s.)
SG16	A	Pale-green paint and plaster (reworked area?)	OM, CL, SEM-EDS, $\mu$ -Raman (t.s.)
SG17	A	Porphyry-like paint and plaster	OM, CL, SEM-EDS, $\mu$ -Raman (t.s.)
SG23A	A	Plaster	OM, CL, SEM-EDS, $\mu$ -Raman (t.s.)
SG25	D	Pale-blue paint on a red–brown layer (morellone?) and plaster	OM, CL, SEM-EDS, $\mu$ -Raman (t.s.)
SG35	D/E	Green layer	EPR (f.)
SG36	D/E	Light-blue layer	EPR (f.)
SG39B	Vault	Blue paint on a red–brown layer (morellone?) and plaster	OM, CL, SEM-EDS, $\mu$ -Raman (t.s.)
SG40	Vault	Filling mortar	OM, CL, SEM-EDS, $\mu$ -Raman (t.s.)
SG46	C	Plaster with remains of a brown preparation layer	OM, CL, SEM-EDS, $\mu$ -Raman (t.s.)
SG47	A	Plaster with remains of a brown preparation layer	OM, CL, SEM-EDS, $\mu$ -Raman (t.s.)

## 2.2. Methods

In Table 1, the analytical methods applied to the samples are reported for identifying the stratigraphy and petrographic characteristics of the plaster, the composition of the binder, the pigments, and the alteration products.

Cross-sections for the microstratigraphic analysis were prepared from sixteen samples (SG9A, SG9B, SG10, SG11, SG12, SG13, SG14, SG15, SG16, SG17, SG23A, SG25, SG39B, SG40, SG46, SG47) at the Department of Earth Sciences at the University of Pisa. The observation of the thin sections was performed using a ZEISS AxioPlan polarized light microscope (OM). For the preparation of the cross-sections, the samples were first observed under a ZEISS STEMI 305 stereo microscope in order to decide the position and direction of the cut and highlight all the layers of the samples, from the surface to the deepest part.

A first set of eight samples (SG9A–B, SG10, SG11, SG12, SG13, SG14, SG15) was investigated at the Department of Geo–environmental and Earth Sciences of the University of Bari Aldo Moro, with the following instrumentation and analytical conditions.

Scanning electron microscope (SEM) observations were made on thin sections, previously fixed on aluminum specimen holders and coated with graphite. An SEM EVO-50XVP (LEO), equipped with an Oxford Instruments AZTEC EDS microanalysis system with SD X-Max<sup>N</sup> detector (80 mm<sup>2</sup>), was used. The accuracy of the analytical data was verified using various standards produced by Micro-Analysis Consultants Ltd. (St. Ives, UK). The working voltage was 15 kV and the beam current between 250 and 400 pA. Spectra acquisitions lasted 50 s, with counts ranging from 25,000 to 30,000. Chemical maps were acquired with a dwell time of 100  $\mu$ s, counting time of 10 min, and a resolution of 2048.

A second set of ten samples was analyzed at the University of Padova, eight at the Department of Geosciences (SG16, SG17, SG23A, SG25, SG39B, SG40, SG46, and SG47), and two, without any preliminary preparation, at the Department of Chemical Sciences (SG35 and SG36).

The samples investigated at the Department of Geosciences were prepared as polished stratigraphic thin sections and analyzed by cathodoluminescence microscopy (CL),  $\mu$ -Raman, and SEM after C coating. The CL analyses were performed with an optical microscope Nikon Labphot2 Pol (with long-working-distance objectives providing 4 $\times$ , 10 $\times$ , and 40 $\times$  magnification) equipped with a CCL (Cold Cathode Luminescence) 8200 mk3; in standard analytical conditions, voltage is 20 kV and beam current is about 200  $\mu$ A. For the  $\mu$ -Raman analyses, the microscope used was a Raman Thermo Scientific DXR with 532 nm laser, 50 $\times$  long-working-distance objective, 3 mW power, 25  $\mu$ m pinhole, and frequency range between 100 and 3500  $\text{cm}^{-1}$ . The SEM analyses were performed with a microscope CamScan MX2500 with W source, detector of secondary and back-scattered electrons, and EDAX EDS (energy-dispersive spectroscopy) microanalysis; the analytical conditions were 25 kV voltage and 15 to 25 mm working distance.

The samples investigated at the Department of Chemical Sciences were analyzed by X-Band CW-EPR spectroscopy. The fragments were placed in a quartz tube as sample holder (3 mm inner diameter, 4 mm outer diameter) and examined at room temperature with a Bruker ECS106 instrument, equipped with a TE102 cavity. Spectra were acquired with 10 scan, modulation amplitude of 0.5 mT, field sweep of 160 mT, and center field of 320 mT. Microwave power was set to 20 mW and microwave frequency was 9.538 GHz. A short  $\mu$ -Raman characterization of the back and front of the two samples was carried out using a Renishaw InVia Spectrometer with laser at 514 nm, objectives 10 $\times$  or 20 $\times$ , 10 s integration time, 50% total output power.

### 3. Results

#### 3.1. Petrography (OM, CL)

The photomicrographs of all the thin sections analyzed are included in Figures 2 and 3. The preparation layer of the painted surface appears to be made up, in all the samples analyzed, of a lime and sand plaster, on which is superimposed a layer of lime, probably applied “a fresco”, pigmented with yellow and red ochres. In the case of red ochres, these are always associated with the presence of C black, while this association is sporadic in yellow ochres. The pigmented layer has a thickness between 7 and 30  $\mu$ m in all samples except for sample SG11, where it exceeds 75  $\mu$ m. From the analyzed cross-sections, the primary color application is carried out with red and yellow ochre also containing a C black pigment. This draft was given with the fresco technique. Subsequently, other colored layers were added (green, yellow, blue, and white), in which the use of a “tempera” technique is likely.

Sample SG40 bears witness to a phase of remaking/rethinking where the previous draft with a very thin layer of red ochre and C black is at the base, which is superimposed on a thin layer pigmented in blue and is covered with a plaster free of aggregate on which there is a new color draft with yellow ochres. Inside the *intonachino* that separates the two phases, there are some granules of a blue pigment and red ochre.

The CL analyses supported the previous observations by providing elements for characterizing the plaster substrates and discriminating the composition of binder and aggregate based on the characteristic luminescence of the different minerals. The observations pointed out that the plaster is generally composed of a lime binder with aggregates of quartz, alkali-feldspars, and plagioclases in various proportions, with minor amounts of carbonate minerals. The aggregate is, in most cases, moderately to poorly sorted.

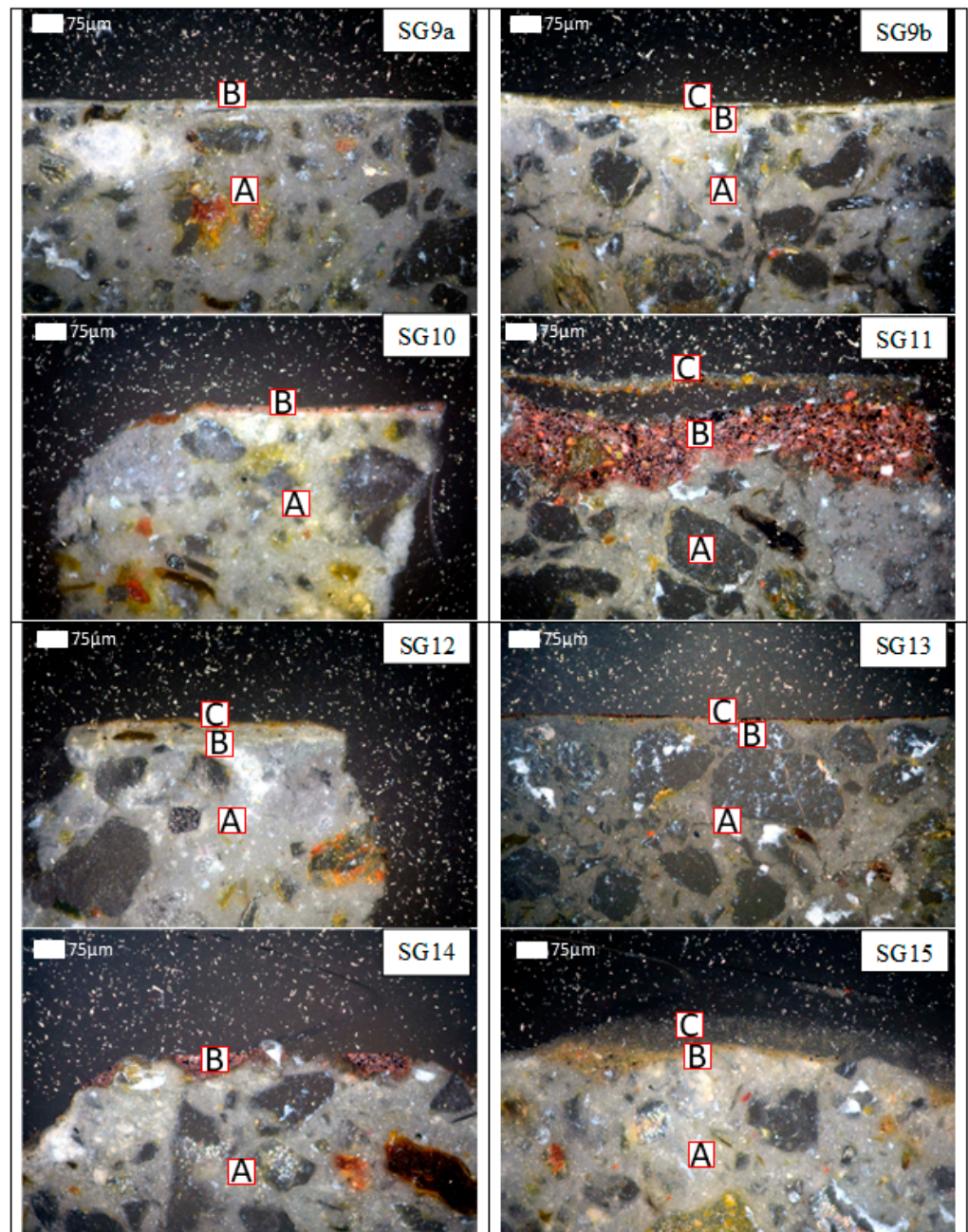


**Figure 2.** Microphotographs of thin sections of the samples SG9a, SG9b, SG10, SG11, SG12, SG13, SG14, and SG15. The capital letters “A”, “B”, and “C” indicate the different layers visible in cross-section, with “A” being the innermost (the plaster) and the others (mostly pigmented) ordered by decreasing depth.

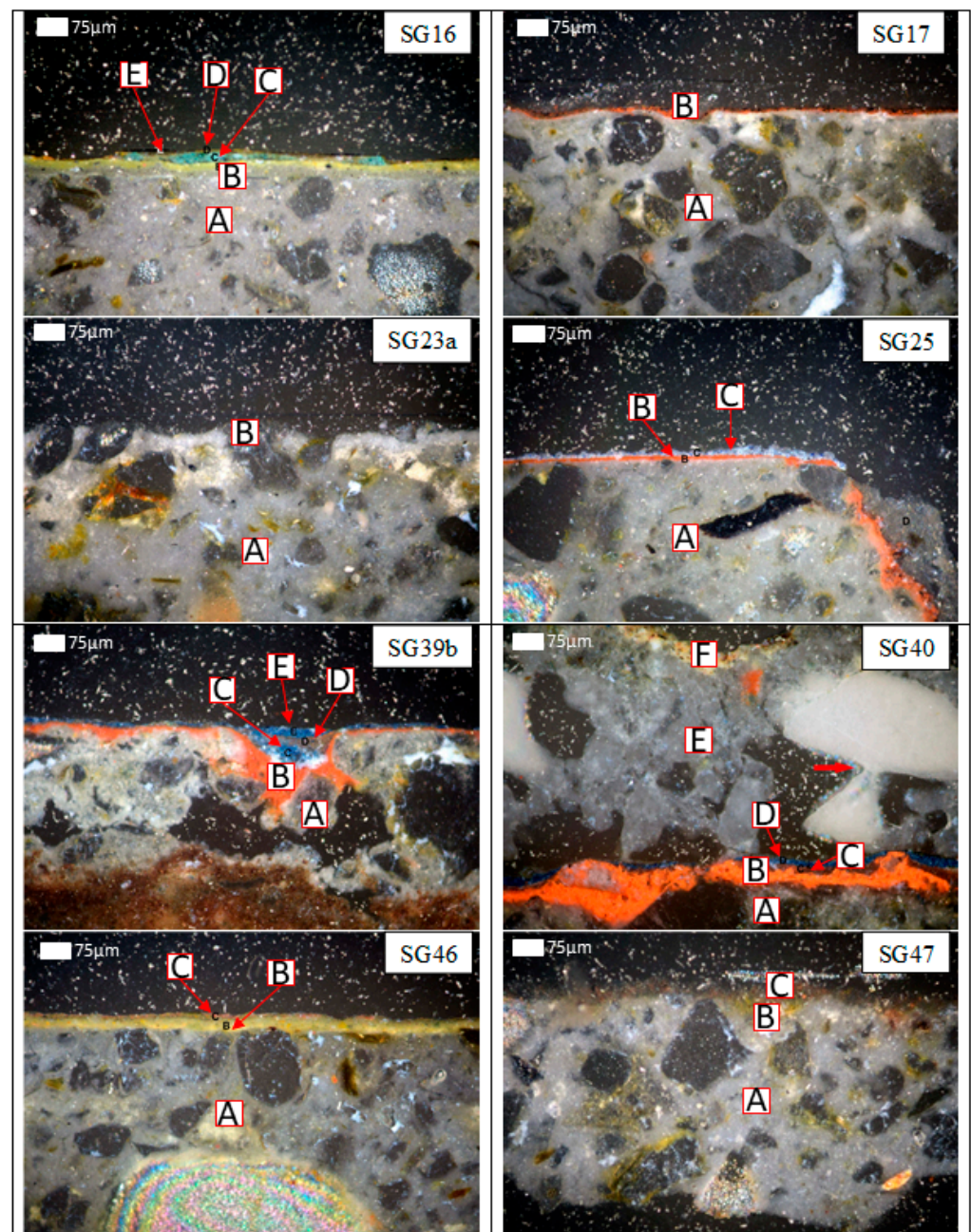


**Figure 3.** Microphotographs of thin sections of the samples SG16, SG17, SG23a, SG25, SG39b, SG40, SG46, and SG47. The capital letters “A”, “B”, “C”, “D”, “E”, and “F” indicate the different layers visible in cross-section, with “A” being the innermost (the plaster) and the others (mostly pigmented) ordered by decreasing depth. Sample SG40 shows a break between the layers consisting of highly purified plaster (E) in which remnants of a blue pigment can be seen (indicated by the red arrow), probably due to the use of a dirty brush or the mixing of pigments from the underlying layer (D).

### 3.2. SEM-EDS and $\mu$ -Raman

The paint layers of the three samples from Panel A (SG16, SG17, and SG47) share the same main pigment, that is, ochre, either red (hematite) and/or yellow (goethite), applied on the plaster “a fresco”. This is suggested by the absence of microstructural discontinuities between the plaster and the paint traces. Generally, the ochres are mixed with fine particles of C black. The stratigraphy of sample SG16 is worthy of further remarks since it is the only one showing “a secco” layers, with additional pigments applied on the dry plaster (Figure 4): one green–blue middle layer made of malachite and one yellow–brown surface

layer probably composed of Cr yellow (because of the detection of Pb chromate grains); this last identification, however, needs to be taken with reservation. Finally, the SEM-EDS analyses of sample SG47 also highlighted the presence of gypsum particles and several surface irregularities and detachments.

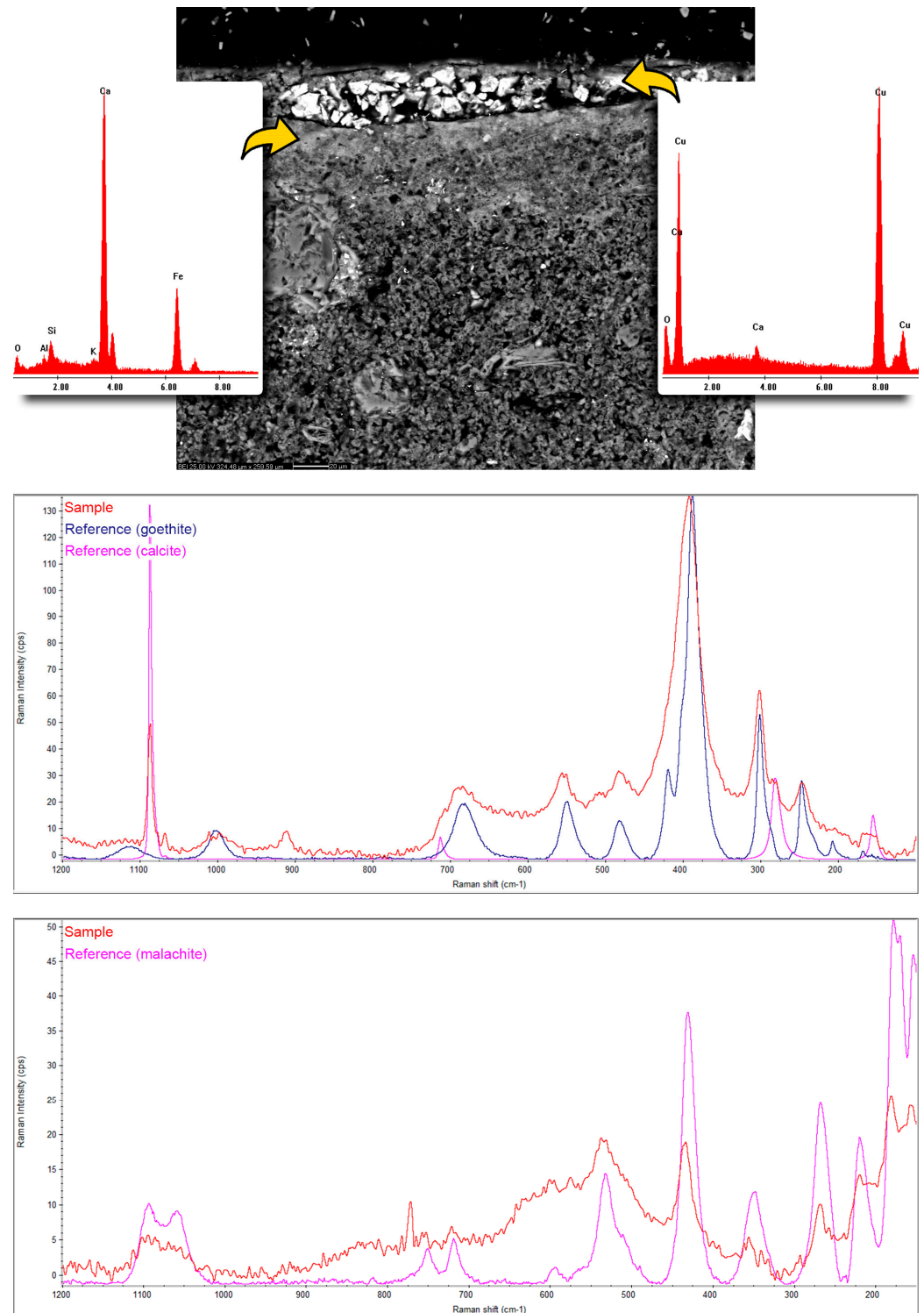


**Figure 4.** Sample SG16: SEM-BSE image with associated SEM-EDS spectra from the spots indicated, and  $\mu$ -Raman spectra calculated on two different paint layers (actual analyses in red, reference spectra from mineral databases in blue and pink).

The SEM-EDS analysis revealed similar microstructural and compositional characteristics for samples SG9A and SG9B. The samples are layered, with an air lime-based arenaceous plaster (A) on which two paint layers (B, ca. 20  $\mu\text{m}$ ; C, ca. 8  $\mu\text{m}$ ) are visible (Figure 5). A detachment is observed between layers B and C. Layer B is more compact than C and both are air lime-based. The EDS microanalysis of the small areas of the painted layers reports the presence of iron oxyhydroxides in layer B, and calcium phosphate (bone black), zinc oxide, and iron oxyhydroxides as pigments in layer C. The compositional traverse in Figure 5 shows the gradual diffusion of phosphorus in the underlying layer, confirming the hypothesis of an “a fresco” painting. The correlation between K, Al, Si, and Fe in layer C might indicate the presence of red bolus [34]. S is due to the presence of gypsum.

Additionally, in SG10, two lime-based layers are visible. Layer B is ca. 20  $\mu\text{m}$  thick and pigmented with hematite. On layer B, an additional pigmented layer (C) partially detached from the previous was recognized, with a thickness of less than 10  $\mu\text{m}$  (Figure 6).

The two samples of Panel B (SG11 and SG12) show two painted layers applied on an air lime-based arenaceous plaster (A). In SG11, layer B can be distinguished by its content of calcium phosphate, zinc oxide, red ochre, and gypsum. Replicated measurements on two other detail areas on layers B and C of the same fragment provided similar data. The binder in layer C is probably of organic origin.

Sample SG12 is layered, with an air lime-based arenaceous plaster (A) on which a B layer is visible in adhesion and a laterally discontinuous C layer. The presence of Mn in the Fe-rich particles in layer B may indicate the use of Sienna, whereas layer C is a lime paint with red ochre. Some gypsum was also identified in this last layer.

In Panel C, SG13 is stratified, with an arenaceous lime plaster (A) on which there are two painted layers. Layer B has a gradual stratigraphic contact with A and sharp contact with C. The EDS chemical mapping shows a high P content in layer C due to some calcium phosphate. Ochre is present in both layer B and layer C.

The painted surface of sample SG46 is also composed of ochre; in this case, however, the yellow ochre (goethite) and red ochre (hematite) are not mixed, with the former composing the “a fresco” bottom layer, and the latter, the upper “a secco” layer, also including scattered C black particles. The upper layer also recorded SEM signals of S and Cl. From a microstructural point of view, the sample shows a distinct surface microcracking, with fractures expanding across the paint layers or partially separating them from the plaster substrate.

The sample from Panel D (SG25) again has red ochre (hematite with some parts of magnetite) as the pigment originally used for the “a fresco” layer. The upper layer, probably applied “a secco”, is blue and made of a combination of ultramarine and Ti white, suggested by the detection of the phases lazurite and rutile; some broad Raman peaks (from about 1300 to 1500  $\text{cm}^{-1}$ ) also point out the presence of organic matter. The SEM microanalyses also revealed the presence of baryte. Finally, another layer, differently oriented in respect to the others (that is, not observed on the surface but sinking into the plaster), is formed of S and Ca (gypsum?) and covers an inner thin red film; although this has the same color as the red ochre layer and is also in direct contact with the substrate, its composition is slightly different, with frequent SEM-EDS signals of Fe, Pb, and Ba from baryte.

SG14 and SG15 were sampled from Panel E. In the first case, layer B is present discontinuously on layer A. The stratigraphic contact is sharp, with complex geometry. The binder of the plaster (A) is air lime. Chemical mapping reveals the presence of Ca phosphate, Zn oxide, and ochre (Figure 7). In the second case, layer B identified by optical microscopy shows no clear separation from layer A. There, Fe enrichment and carbonaceous inclusions are detected. The outer surface of B also shows the presence of gypsum. Layer C is poorly preserved and consists of gypsum and calcite.

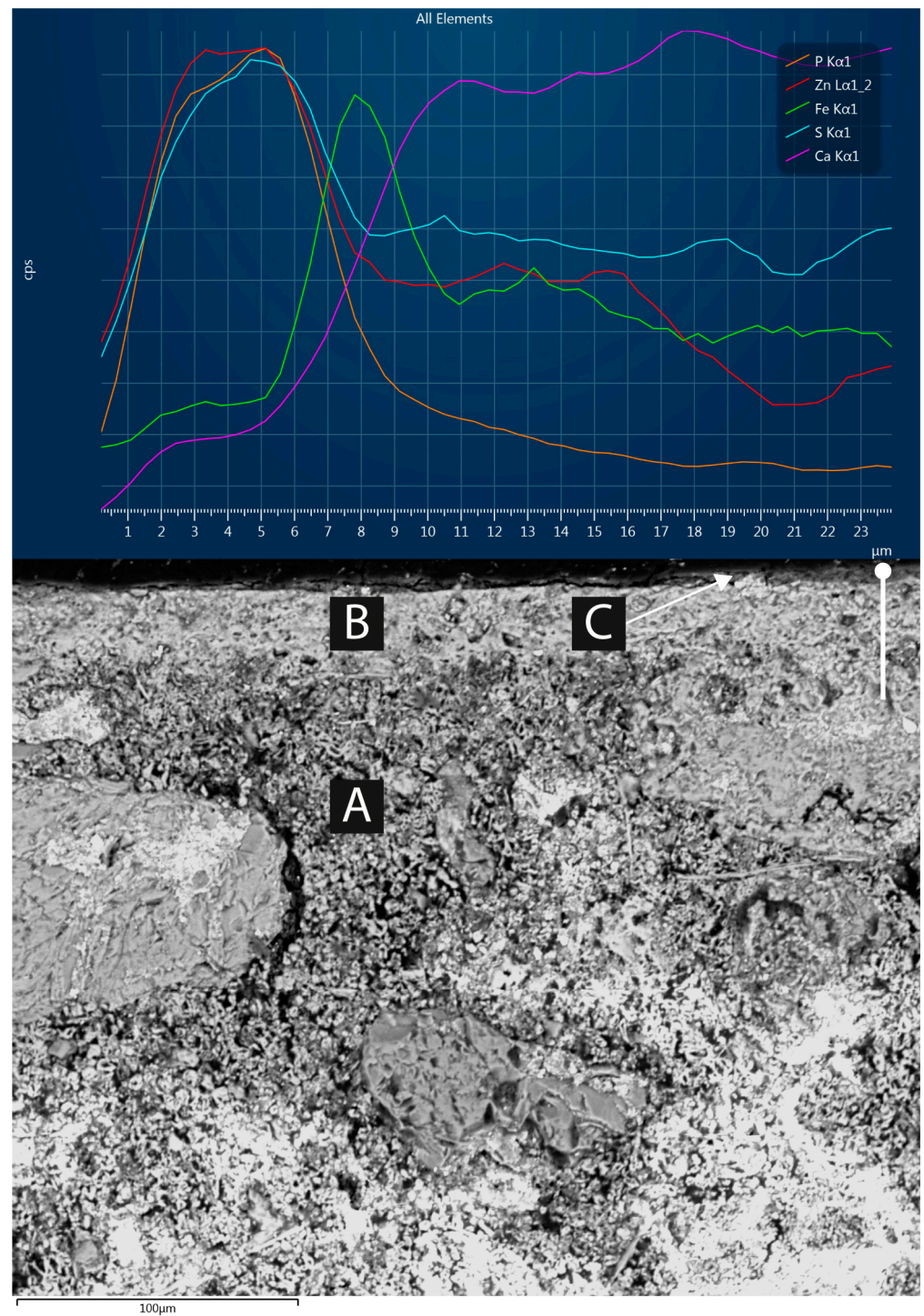


**Figure 5.** SG9A, SEM-BSE image (bottom) of the outer portion of the sample (plaster layer “A” and paint layers “B” and “C”) and the EDS traverse across the identified layers (top). The intensities of the K and L lines of the elements in the legend are normalized to better detect lateral variation in the painted layers.

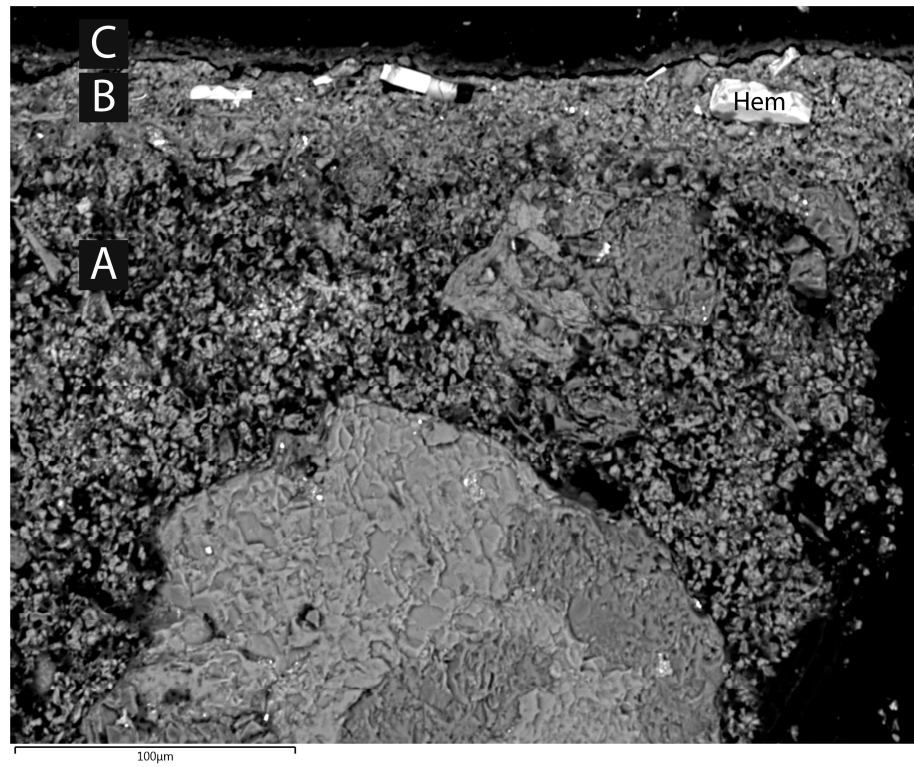


**Figure 6.** SG10, SEM-BSE image of the outer portion of the sample (plaster layer “A” and paint layers “B” and “C”). Light grey tabular fragments of hematite (Hem) occur as pigment in layer B.

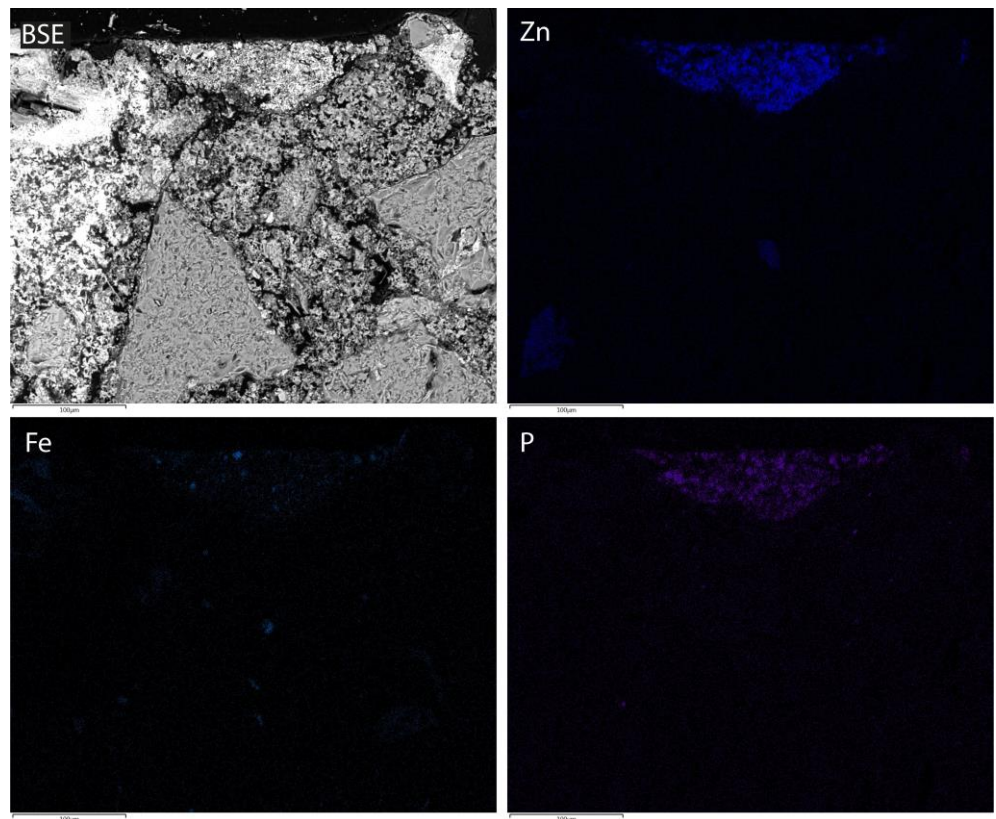


**Figure 7.** SG14, SEM-BSE image of the outer portion of the sample and related EDS maps of Zn, Fe, and P.

The sample from Panel “sky” (SG23A) is a non-painted plaster fragment.

The samples from the vault (SG39B and SG40) are the most complex compositionally, considering their stratigraphy composed of six layers. Sample SG39B has four different paint layers above the plaster substrate: the first and deepest, applied “a fresco”, is made of red ochre (hematite with magnetite); the second, applied “a secco”, is blue and made of azurite (with traces of Zn and As)—it is detectable only in a very small area and never on the exposed surface; the third, more continuous but almost colorless, has an ambiguous composition, enriched in gypsum (from the SEM signals of S and Ca) and resins or organic polymers (from the  $\mu$ -Raman spectra); finally, the fourth, the most superficial, covers the entire surface and is blue and composed of ultramarine (lazurite), with traces of Pb particles (pointing out the possible mix of ultramarine with Pb white) and Ba (probably baryte) (Figure 8). With regard to sample SG40, this is formed by two main stratigraphic domains. The first has a sequence of three layers overlying the plaster substrate: from bottom to top, one red “a fresco” film composed of cinnabar, one layer rich in gypsum and resins or organic polymers, and one blue “a secco” layer with ultramarine (lazurite) mixed with Pb white (basic Pb carbonate) with baryte traces. The second overlaying stratigraphic domain consists of an additional lime plaster layer (much more porous and with nearly just lime, without the silicate aggregate) and one final yellow–brown paint film made of yellow ochre (goethite) mixed with C black grains, applied “a fresco” on the surface. The surface also records the presence of gypsum.

### 3.3. EPR

CW-EPR was applied on two small fragments (SG35 and SG36) to evaluate if this technique could provide further information on specific aspects of the samples; EPR is able to spot paramagnetic defects (color centers, radicals) or paramagnetic metals ( $\text{Cu}^{2+}$ ,  $\text{Mn}^{2+}$ ,  $\text{Fe}^{3+}$ ), which are commonly present in many pigments and materials as substitutional ions. EPR is a bulk technique, so the whole sample is examined and specific pieces of information related to the different painted layers are not accessible.

A preliminary overview of the two fragments, front and back, was conducted using optical microscopy and Raman spectroscopy.

The SG35 front (Figure 9) is characterized by a layer with small blue grains on a yellow background giving a green hue. Some bigger blue grains can be spotted, which Raman identifies unambiguously as azurite. On the back, pale green crystals are present, which Raman identifies likely as a combination of brochantite (basic copper sulfate) and atacamite (basic copper chloride), which are likely alteration by-products from an original copper-based pigment. Two unidentified peaks at 444 and 1475  $\text{cm}^{-1}$  suggest the presence of some other compound.

The EPR spectrum of SG35 (Figure 10) is characterized by a sharp signal, whose  $g$ -factor ( $g = 2.0035$ ) is related to a C radical, likely a radical in C black. A six-line pattern is also observed, attributable to  $\text{Mn}^{2+}$  in Ca carbonate, and a signal at  $g \sim 2.06$ , with linewidth  $H_{pp} = 4.3$  mT can be attributed to  $\text{Cu}^{2+}$  in some compounds deriving from the alteration of a copper-based pigment. In azurite, brochantite, and atacamite (the copper-based pigments detected by Raman), the  $\text{Cu}^{2+}$  ions are either antiferromagnetically coupled or have very broad EPR lines; therefore, the  $g \sim 2.06$  signal is unlikely to be related to these latter and could be attributed to some complex of copper with an organic compound.

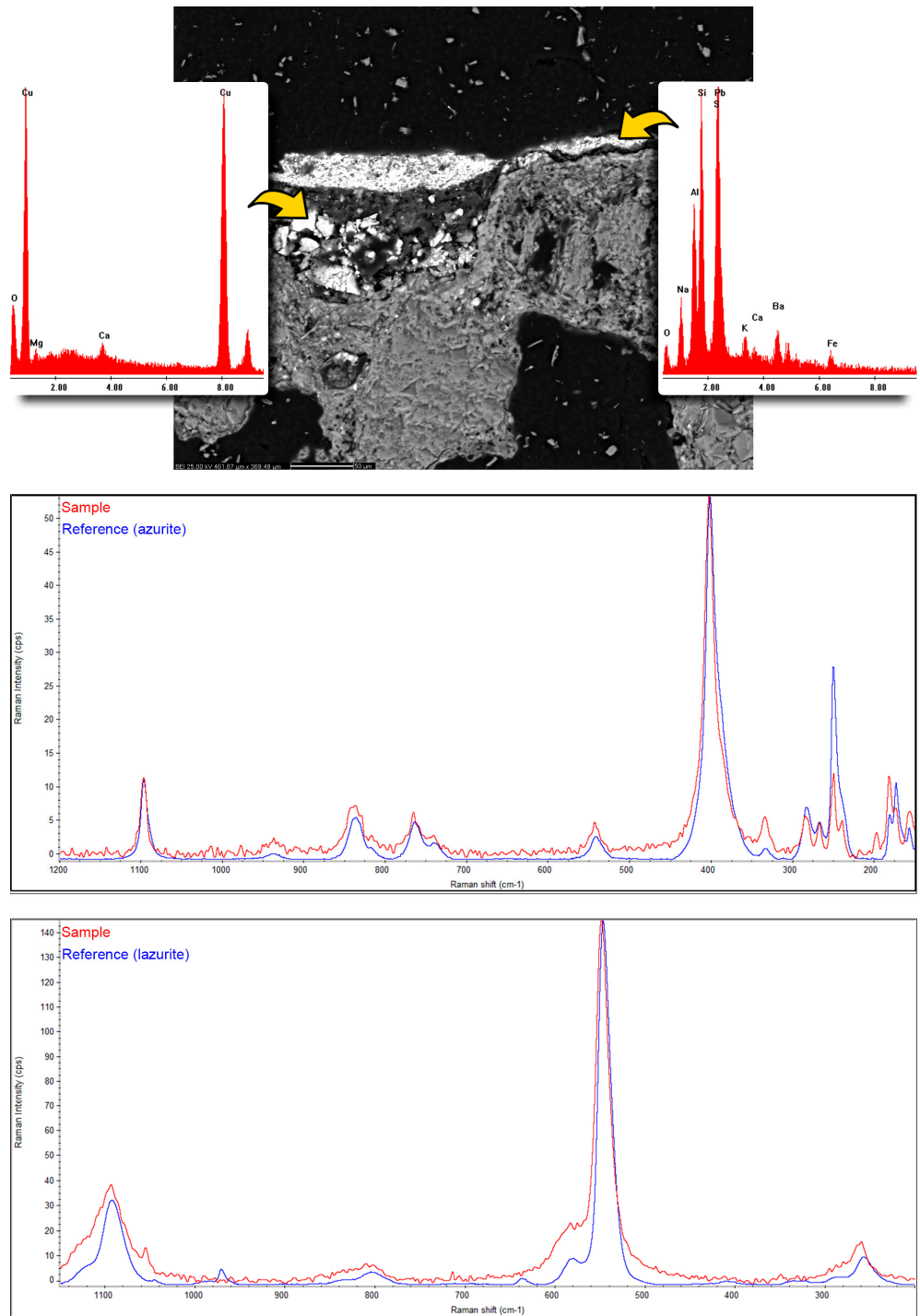


**Figure 8.** Sample SG39B: SEM-BSE image with associated SEM-EDS spectra from the spots indicated, and  $\mu$ -Raman spectra calculated on two different paint layers (actual analyses in red, reference spectra from mineral databases in blue).

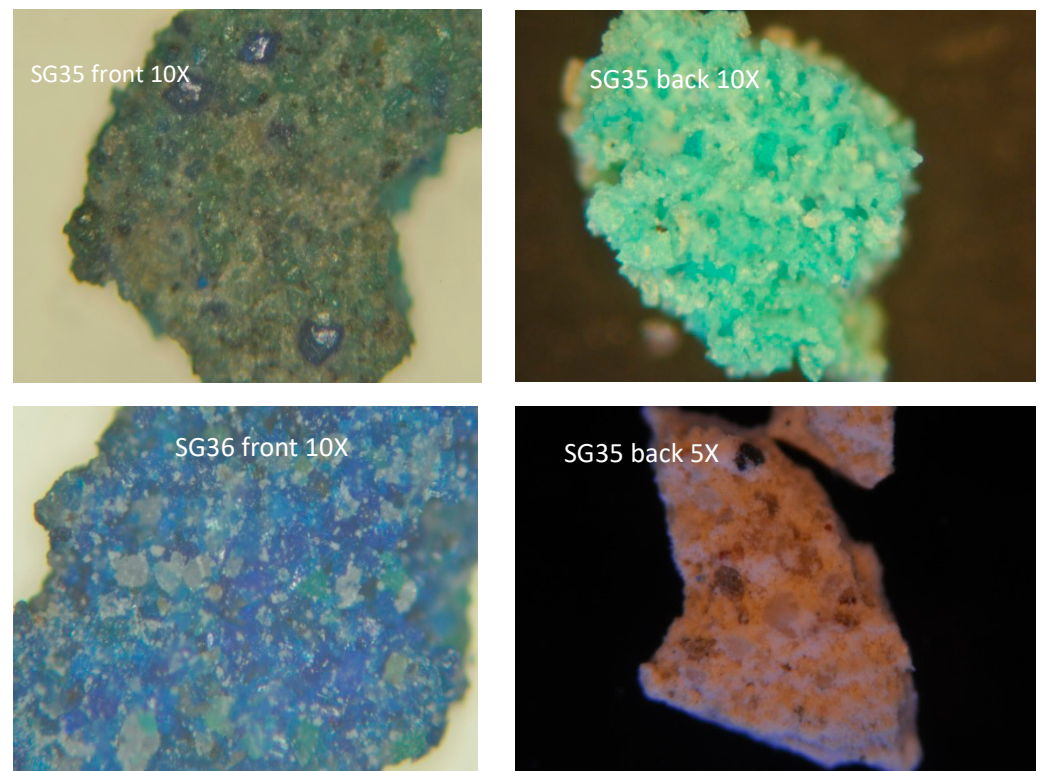


**Figure 9.** Above: SG35 front (left) and back (right). Below: SG36 front (left) and back (right).

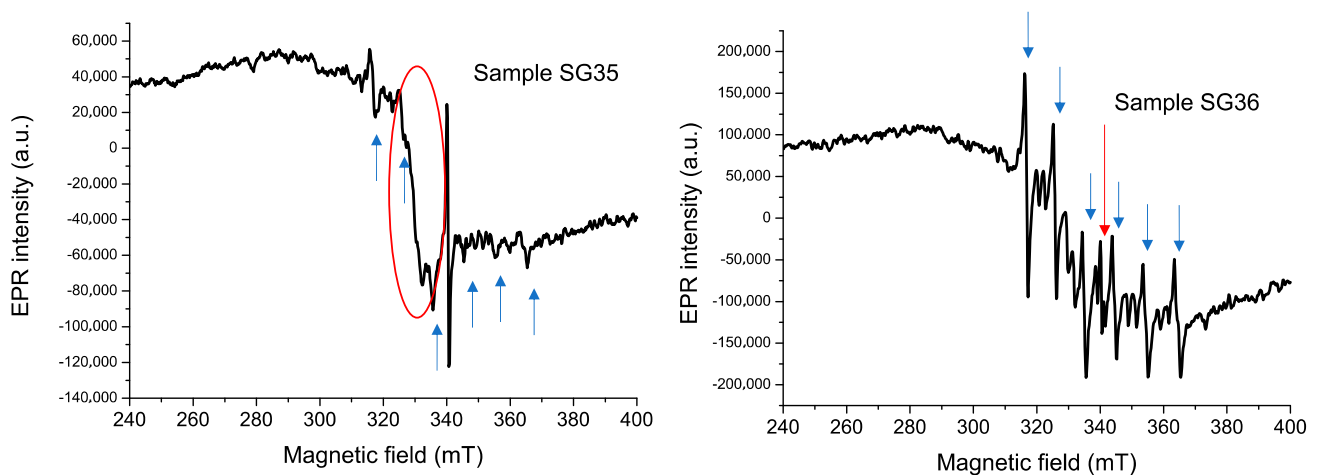


**Figure 10.** Left: EPR of SG35. Red asterisk marks the sharp signal of a C radical; blue arrows mark the sextet of  $\text{Mn}^{2+}$ ; the red circle highlights the signal of  $\text{Cu}^{2+}$ . Right: EPR of SG36. Red arrow marks a C radical; blue arrows mark the sextet of  $\text{Mn}^{2+}$ .

The SG36 front is uniformly covered by blue grains, which Raman identifies again as azurite. The SG36 back is yellow–red on a white background; only peaks due to calcium carbonate are observed in the Raman spectrum.

In the EPR spectrum of sample SG36, no  $\text{Cu}^{2+}$  signal is observed, while a strong  $\text{Mn}^{2+}$  six-line pattern is seen, again attributable to manganese in Ca carbonate. The signal is stronger than in SG35. The C black radical signal is also seen, although weaker than in SG35. Both SG35 and SG36 present a broad background signal attributable to iron oxyhydroxides.

## 4. Discussion

### 4.1. Stratigraphy: Original and Successive Interventions

The samples analyzed showed stratigraphic and compositional similarities, summarized in Table 2. A common substratum of lime plaster with similar composition was identified in all the samples. The paint layers show a more or less complex stratification according to the pictorial intention of the artist and the further restorations.

**Table 2.** Summary of the results obtained. The question marks indicate doubtful interpretations requiring in-depth validation. Pigments of past restorations are reported in italics.

Sample	Layer A (Plaster)	Layer B	Layer C	Layer D	Layer E	Layer F
SG9A		red bolus	bone black	/	/	/
SG9B		red bolus	<i>bone black, red bolus, ZnO</i>	/	/	/
SG10		hematite, C black	<i>red bolus, ZnO</i>	/	/	/
SG11		<i>bone black, red ochre, ZnO</i>	<i>organic?</i>	/	/	/
SG12	Air lime with quartz, alkali-feldspars, and plagioclases, micas with minor carbonates as aggregate	C black, sienna	/	/	/	/
SG13		C black, ochre	bone black, ochre	/	/	/
SG14		<i>bone black + ochre + ZnO</i>	/	/	/	/
SG15		C black + ochre	/	/	/	/
SG16		yellow ochre + C black	malachite	<i>Cr yellow?</i>	/	/
SG17		red ochre + C black	/	/	/	/
SG23A		/	/	/	/	/
SG25		red ochre	<i>ultramarine + Ti white</i>	/	/	/
SG35		azurite <sup>1</sup>		/	/	/
SG36		azurite		/	/	/
SG39B		red ochre	azurite	<i>resins/org. polymers?</i>	<i>ultramarine + Pb white</i>	/
SG40		cinnabar	<i>resins/org. polymers?</i>	<i>ultramarine + Pb white</i>	lime plaster	yellow ochre + C black
SG46		yellow ochre	red ochre + C black	/	/	/
SG47		yellow ochre + C black	red ochre	/	/	/

<sup>1</sup> Altered in brochantite/atacamite.

The stratigraphy shows a combination of “a fresco” and “a secco” techniques [35,36] in almost all the samples, as supported by the thickness of the layers and carbonation of the surfaces [37,38]. Further details about the technology are reported in Section 4.2. Most of the samples show traces of past restoration (Table 2), as also observed by other authors in different samples of the same panels [39–42].

Other compounds not relatable to actual pigments or dyes are the resins and organic polymers often detected in thick layers on the surface of the samples. These may trace back to finishing touches or restoration works [43].

### 4.2. Lime Plasters: Raw Materials and Technological Aspects

The plasters (layer A) are classifiable as air lime (CaO > 97 wt. %) mortars with an arenaceous texture. The absence of calcination relics and slacking nodules points to an accurate preparation of the lime putty. The aggregate consists of mono- and polycrystalline quartz, alkali-feldspars, plagioclases, micas, Fe aggregates, and minor carbonates. The texture is unimodal to seriate, mainly in the range of fine sand. These petrographic features point to fluvial fine sand (Torrente Raio?) used as aggregate (Figures 2 and 3) and are compatible with the siliciclastic composition of the turbiditic complex in the area of Tornimparte [44]. The lime/aggregate ratio of about 1:1 allowed workability and a

smoother and denser plaster. Contrary to what is reported in various medieval treatises, the plaster intended to receive the color does not contain marble or spathic calcite powder as part of the aggregate [45].

#### 4.3. Pigments, Binders, and Painting Techniques

Red and yellow ochres were found as the main pigments in the deeper pictorial layers in most samples (layers B, C: samples SG9-SG15, SG16, SG17, SG25, SG39B, SG46, and SG47). These layers were likely applied “a fresco”, as indicated by the analysis of the SG16 sample. C black was also detected in many of these inner layers. External pictorial layers (C, D) often presented more recent pigments of different colors, sometimes applied “a secco”. For example, malachite and maybe Pb chromate were detected in SG16, ultramarine and Ti white in SG25, ultramarine and azurite in SG39B, and ultramarine and Pb white in SG40. In many samples, the occurrence of Ca sulfate, likely an alteration product, was inferred by the presence of S and Ca in the SEM-EDS analysis (Section 4.3). In addition, the presence of polymeric organic compounds was supposed by the Raman analyses in two samples (SG40, SG25). It is worth noting that SG9 and SG10 have a layer containing Ca phosphate (bone black) and Zn oxide present as probable materials from later interventions. In SG35, the EPR analysis detects signals due to C black radicals and copper alteration products; in SG36, the EPR signal was detected due to Mn (II) in Ca carbonate.

The frequent presence of ochre and C black in fresco layers may be attributed to the primary design made with only red and yellow ochre (e.g., sample SG47), to which layers of other colors are superimposed (blue, green, yellow, black, and white), made with an “a secco” technique. In particular, the use of C black is typical for the dusting technique, for the realization of the sketch of the drawing, or to darken the hue of other colors.

Some microchemical characteristics observed on the stratigraphic thin sections allow for making hypotheses on Saturnino Gatti’s preferred painting technique when working on his frescoes in Tornimparte. For example, the identification of frequent “a secco” layers, evident from the lack of blending between pigment grains and plaster and the presence of sharp but plain discontinuities, points out a two-step working technique, with the artist tending to apply color corrections on the dry plaster. In others (e.g., sample SG39B), pigment traces localized only in specific areas or covered by further, different paint films, may point out mistakes or reworks, or even second thoughts on the pigment choice—as for azurite, detected only in such contexts.

#### 4.4. Alteration and Decay

The most recurring phase linked to the alteration of the painted walls is gypsum (e.g., samples SG25, SG39B, SG40, SG46, SG47, etc.). Minor traces of baryte and chlorides were also detected. Those alteration products may be frequently associated with surface microcracking and disintegration because of cyclic processes of salt weathering: the secondary phases crystallize and dissolve below and within the paint films, produce subflorescences, and exert localized pressures and mechanical stresses.

The EPR spectra acquired on two samples, SG35 and SG36, indicate that the technique could be useful in the identification of copper alteration by-products, deriving from chemical interaction between  $\text{Cu}^{2+}$  and organic binders (e.g., in the “a secco” azurite layers). Additionally, C radicals could be spotted. These products can have a role in fresco degradation, and therefore, their identification has some interest.

### 5. Conclusions

The petrographic and chemical analysis of a selection of samples from the Church of San Panfilo revealed some significant information about the technology and past restorations of Gatti’s frescoes. Summing up, all the samples are characterized by a base layer of plaster and up to five pictorial layers. The layers containing ochres, raw sienna, C black, and cinnabar are related to the original fresco. The pigments associated with additions or past restorations are red bolus, bone black, ZnO, ochre, ultramarine, azurite, malachite,

whites (Pb or Ti), and yellows (Pb and Cr?). The preparation of lime plaster was based on the calcination of local Mesozoic limestones and the use of siliciclastic fluvial sand. The absence of slaking lumps points to the use of aged lime putty as a binder.

These findings, seen in the broader picture of the work conducted by all the Italian research groups involved in this AIAR's national project, have a double value: they help to comprehend the past better, providing insights into the creation process and history of Saturnino Gatti's frescoes; and they preserve it knowingly in the future, giving precious scientific and technical diagnostic information for the restorations soon to begin.

**Author Contributions:** Conceptualization, G.E. and L.G.; investigation, G.E., M.L., S.P., L.G., C.M., M.S. and L.C.G.; resources, G.E., M.L. and C.M.; writing—original draft preparation, G.E., L.G., S.P. and A.Z.; writing—review and editing, G.E., A.M., C.M. and M.L.; visualization, G.E., S.P., L.G. and A.Z.; supervision, G.E. All authors have read and agreed to the published version of the manuscript.

**Funding:** This work was performed in the framework of the Project Tornimparte—"Archeometric investigation of the pictorial cycle of Saturnino Gatti in Tornimparte (AQ, Italy)" sponsored in 2021 by the Italian Association of Archeometry AIAR ([www.associazioneaiar.com](http://www.associazioneaiar.com), accessed on 1 June 2023).

**Data Availability Statement:** All data are in the paper.

**Acknowledgments:** The authors thank Pasquale Acquafredda and Nicola Mongelli for their technical support in SEM analysis. This research benefited from instrumental upgrades of Potenziamento Strutturale PONA3-00369 of the University of Bari Aldo Moro titled "Laboratorio per lo Sviluppo Integrato delle Scienze e delle Tecnologie dei Materiali Avanzati e per dispositivi innovativi (SISTEMA)".

**Conflicts of Interest:** The authors declare no conflict of interest.

## References

1. Arbace, L. I Volti dell'Anima. Saturnino Gatti. In *Vita e Opere di un Artista del Rinascimento*; Paolo De Siena Editore: Pescara, Italy, 2012; ISBN 88-96341-11-6.
2. Zezza, A. Paintings, Frescoes, and Cycles. In *A Companion to the Renaissance in Southern Italy (1350–1600)*; Di Vitiis, B., Ed.; Brill: New York, NY, USA, 2022; pp. 591–617. ISBN 978-90-04-52637-2.
3. Vittorini, A. L'Aquila 2009–2019: Back to the Future. Cultural Heritage and Post-Seismic Reconstruction Challenges. In *Invisible Reconstruction. Cross-Disciplinary Responses to Natural, Biological and Man-Made Disasters*; Patrizio Gunning, L., Rizzi, P., Eds.; Fringe; UCL Press: London, UK, 2022; pp. 11–28.
4. Quagliarini, E.; Lenci, S.; Seri, E. On the Damage of Frescoes and Stuccoes on the Lower Surface of Historical Flat Suspended Light Vaults. *J. Cult. Herit.* **2012**, *13*, 293–303. [[CrossRef](#)]
5. Lermé, N.; Hégarat-Masclé, S.L.; Zhang, B.; Aldea, E. Fast and Efficient Reconstruction of Digitized Frescoes. *Pattern Recognit. Lett.* **2020**, *138*, 417–423. [[CrossRef](#)]
6. Bruno, N.; Mikolajewska, S.; Roncella, R.; Zerbi, A. Integrated Processing of Photogrammetric and Laser Scanning Data for Frescoes Restoration. *Int. Arch. Photogramm. Remote Sens. Spat. Inf. Sci. ISPRS Arch.* **2022**, *46*, 105–112. [[CrossRef](#)]
7. Piovesan, R.; Maritan, L.; Amatucci, M.; Nodari, L.; Neguer, J. Wall Painting Pigments of Roman Empire Age from Syria Palestina Province (Israel). *Eur. J. Mineral.* **2016**, *28*, 435–448. [[CrossRef](#)]
8. Pecchioni, E.; Pallecchi, P.; Giachi, G.; Calandra, S.; Santo, A.P. The Preparatory Layers in the Etruscan Paintings of the Tomba dei Demoni Alati in the Sovana Necropolis (Southern Tuscany, Italy). *Appl. Sci.* **2022**, *12*, 3542. [[CrossRef](#)]
9. Mangone, A.; Colombi, C.; Eramo, G.; Muntoni, I.M.; Forleo, T.; Giannossa, L.C. Pigments and Techniques of Hellenistic Apulian Tomb Painting. *Molecules* **2023**, *28*, 1055. [[CrossRef](#)]
10. Holclajtner-Antunović, I.; Stojanović-Marić, M.; Bajuk-Bogdanović, D.; Žikić, R.; Uskoković-Marković, S. Multi-Analytical Study of Techniques and Palettes of Wall Paintings of the Monastery of Žiča, Serbia. *Spectrochim. Acta Part A Mol. Biomol. Spectrosc.* **2016**, *156*, 78–88. [[CrossRef](#)] [[PubMed](#)]
11. Miriello, D.; Bloise, A.; Crisci, G.M.; De Luca, R.; De Nigris, B.; Martellone, A.; Osanna, M.; Pace, R.; Pecci, A.; Ruggieri, N. Non-Destructive Multi-Analytical Approach to Study the Pigments of Wall Painting Fragments Reused in Mortars from the Archaeological Site of Pompeii (Italy). *Minerals* **2018**, *8*, 134. [[CrossRef](#)]
12. Garavelli, A.; Andriani, G.F.; Fioretti, G.; Iurilli, V.; Marsico, A.; Pinto, D. The "Sant'Angelo in Criptis" Cave Church in Santeramo in Colle (Apulia, South Italy): A Multidisciplinary Study for the Evaluation of Conservation State and Stability Assessment. *Geosciences* **2021**, *11*, 382. [[CrossRef](#)]
13. Carlomagno, G.M.; Meola, C. Comparison between Thermographic Techniques for Frescoes NDT. *NDT E Int.* **2002**, *35*, 559–565. [[CrossRef](#)]

14. Gusella, V.; Cluni, F.; Liberotti, R. Feasibility of a Thermography Nondestructive Technique for Determining the Quality of Historical Frescoed Masonries: Applications on the Templar Church of San Bevignate. *Appl. Sci.* **2021**, *11*, 281. [[CrossRef](#)]
15. Almaviva, S.; Fantoni, R.; Colao, F.; Puiu, A.; Bisconti, F.; Fiocchi Nicolai, V.; Romani, M.; Cascioli, S.; Bellagamba, S. LIF/Raman/XRF Non-Invasive Microanalysis of Frescoes from St. Alexander Catacombs in Rome. *Spectrochim. Acta Part A Mol. Biomol. Spectrosc.* **2018**, *201*, 207–215. [[CrossRef](#)]
16. Sáez-Hernández, R.; Antela, K.U.; Gallelo, G.; Cervera, M.L.; Mauri-Aucejo, A.R. A smartphone-based innovative approach to discriminate red pigments in roman frescoes mock-ups. *J. Cult. Herit.* **2022**, *58*, 156–166. [[CrossRef](#)]
17. Merello, P.; Beltrán, P.; García-Diego, F.J. Quantitative Non-Invasive Method for Damage Evaluation in Frescoes: Ariadne’s House (Pompeii, Italy). *Environ. Earth Sci.* **2016**, *75*, 165. [[CrossRef](#)]
18. Fioretti, G.; Campobasso, C.; Capotorto, S. Digital Photogrammetry as Tool for Mensiochronological Analysis: The Case of St. Maria Veterana Archaeological Site (Triggiano, Italy). *Digit. Appl. Archaeol. Cult. Herit.* **2020**, *19*, e00158. [[CrossRef](#)]
19. Horgnies, M.; Bayle, M.; Gueit, E.; Darque-Ceretti, E.; Aucouturier, M. Microstructure and Surface Properties of Frescoes Based on Lime and Cement: The Influence of the Artist’s Technique. *Archaeometry* **2015**, *57*, 344–361. [[CrossRef](#)]
20. Helvaci, Y.Z.; Dias, L.; Manhita, A.; Martins, S.; Cardoso, A.; Candeias, A.; Gil, M. Tracking Old and New Colours: Material Study of 16th Century Mural Paintings from Évora Cathedral (Southern Portugal). *Color Res. Appl.* **2016**, *41*, 276–282. [[CrossRef](#)]
21. Vasco, G.; Serra, A.; Manno, D.; Buccolieri, G.; Calcagnile, L.; Buccolieri, A. Investigations of Byzantine Wall Paintings in the Abbey of Santa Maria Di Cerrate (Italy) in View of Their Restoration. *Spectrochim. Acta Part A Mol. Biomol. Spectrosc.* **2020**, *239*, 118557. [[CrossRef](#)]
22. Graziano, S.F.; Rispoli, C.; Guarino, V.; Balassone, G.; Di Maio, G.; Pappalardo, L.; Cappelletti, P.; Damato, G.; De Bonis, A.; Di Benedetto, C.; et al. The Roman Villa of Positano (Campania Region, Southern Italy): Plasters, Tiles and Geoarchaeological Reconstruction. *Int. J. Conserv. Sci.* **2020**, *11*, 319–344.
23. De Benedetto, G.E.; Savino, A.; Fico, D.; Rizzo, D.; Pennetta, A.; Cassiano, A.; Minerva, B. A Multi-Analytical Approach for the Characterisation of the Oldest Pictorial Cycle in the 12th Century Monastery Santa Maria Delle Cerrate. *Open J. Archaeom.* **2013**, *1*, e12. [[CrossRef](#)]
24. Bersani, D.; Berzioli, M.; Caglio, S.; Casoli, A.; Lottici, P.P.; Medeghini, L.; Poldi, G.; Zannini, P. An Integrated Multi-Analytical Approach to the Study of the Dome Wall Paintings by Correggio in Parma Cathedral. *Microchem. J.* **2014**, *114*, 80–88. [[CrossRef](#)]
25. Romani, M.; Capobianco, G.; Pronti, L.; Colao, F.; Seccaroni, C.; Puiu, A.; Felici, A.C.; Verona-Rinati, G.; Cestelli-Guidi, M.; Tognacci, A.; et al. Analytical Chemistry Approach in Cultural Heritage: The Case of Vincenzo Pasqualoni’s Wall Paintings in S. Nicola in Carcere (Rome). *Microchem. J.* **2020**, *156*, 104920. [[CrossRef](#)]
26. Alberghina, M.F.; Schiavone, S.; Greco, C.; Saladino, M.L.; Armetta, F.; Renda, V.; Caponetti, E. How Many Secret Details Could a Systematic Multi-Analytical Study Reveal about the Mysterious Fresco Trionfo Della Morte? *Heritage* **2019**, *2*, 145. [[CrossRef](#)]
27. Crupi, V.; Fazio, B.; Fiocco, G.; Galli, G.; La Russa, M.F.; Licchelli, M.; Majolino, D.; Malagodi, M.; Ricca, M.; Ruffolo, S.A.; et al. Multi-Analytical Study of Roman Frescoes from Villa Dei Quintili (Rome, Italy). *J. Archaeol. Sci. Rep.* **2018**, *21*, 422–432. [[CrossRef](#)]
28. Angelini, I.; Asscher, Y.; Secco, M.; Parisatto, M.; Artioli, G. The Pigments of the Frigidarium in the Sarno Baths, Pompeii: Identification, Stratigraphy and Weathering. *J. Cult. Herit.* **2019**, *40*, 309–316. [[CrossRef](#)]
29. Mohanu, I.; Mohanu, D.; Gomoiu, I.; Barbu, O.H.; Fechet, R.M.; Vlad, N.; Voicu, G.; Truşcă, R. Study of the Frescoes in Ioneştii Govorii Wooden Church (Romania) Using Multi-Technique Investigations. *Microchem. J.* **2016**, *126*, 332–340. [[CrossRef](#)]
30. Hakebyan, Z.A. The Frescoes of Haghat Monastery in the Historical-Confessional Context of the 13th Century. *Actual Probl. Theory Hist. Art* **2021**, *11*, 256–267. [[CrossRef](#)]
31. Luvidi, L.; Prestileo, F.; De Paoli, M.; Riminesi, C.; Del Fà, R.M.; Magrini, D.; Fratini, F. Diagnostics and Monitoring to Preserve a Hypogeum Site: The Case of the Mithraeum of Marino Laziale (Rome). *Heritage* **2021**, *4*, 235. [[CrossRef](#)]
32. Ranalli, G.; Alfano, G.; Belli, C.; Lustrato, G.; Colombini, M.P.; Bonaduce, I.; Zanardini, E.; Abbruscato, P.; Cappitelli, F.; Sorlini, C. Biotechnology applied to cultural heritage: Biorestitution of frescoes using viable bacterial cells and enzymes. *J. Appl. Microbiol.* **2005**, *98*, 73–83. [[CrossRef](#)]
33. Galli, A.; Alberghina, M.F.; Re, A.; Magrini, D.; Grifa, C.; Ponterio, R.C.; La Russa, M.F. Special Issue: Results of the II National Research project of AIAR: Archaeometric study of the frescoes by Saturnino Gatti and workshop at the church of San Panfilo in Tornimparte (AQ, Italy). *Appl. Sci.* **2023**. *to be submitted*.
34. Čiuladienė, A.; Luckutė, A.; Kiuberis, J.; Kareiva, A. Investigation of the Chemical Composition of Red Pigments and Binding Media. *Chemija* **2018**, *29*, 243–256. [[CrossRef](#)]
35. Cennini, C. *Il Libro Dell’arte, o Trattato della Pittura di Cennino Cennini*; Milanese, G., Milanese, C., Eds.; Le Monnier: Florence, Italy, 1859.
36. Mora, P.; Mora, L.; Philippot, P. *La Conservazione Delle Pitture Murali*; Editrice Compositori: Bologna, Italy, 1999.
37. Piovesan, R.; Mazzoli, C.; Maritan, L.; Cornale, P. Fresco and lime paint: An experimental study and objective criteria for distinguishing between these painting techniques. *Archaeometry* **2012**, *54*, 723–736. [[CrossRef](#)]
38. Ergenç, D.; Fort, R.; Varas–Muriel, M.J.; Alvarez de Buergo, M. Mortars and Plasters—How to Characterize Aerial Mortars and Plasters. *Archaeol. Anthr. Sci.* **2021**, *13*, 197. [[CrossRef](#)]
39. Bonizzoni, L.; Caglio, S.; Galli, A.; Lanteri, L.; Pelosi, C. Materials and technique: The first look at Saturnino Gatti. *Appl. Sci.* **2023**, *13*, 6842. [[CrossRef](#)]

40. Bonizzoni, L.; Caglio, S.; Galli, A.; Germinario, C.; Izzo, F.; Magrini, D. Identifying original and restoration materials through spectroscopic analyses on Saturnino Gatti mural paintings: How far a non-invasive approach can go. *Appl. Sci.* **2023**, *13*, 6638. [[CrossRef](#)]
41. Briani, F.; Caridi, F.; Ferella, F.; Gueli, A.M.; Marchegiani, F.; Nisi, S.; Paladini, G.; Pecchioni, E.; Politi, G.; Santo, A.P.; et al. Multi-technique characterization of painting drawings of the pictorial cycle at the San Panfilo Church in Tornimparte (AQ). *Appl. Sci.* **2023**, *13*, 6492. [[CrossRef](#)]
42. Armetta, F.; Giuffrida, D.; Ponterio, R.C.; Falcon Martinez, M.F.; Briani, F.; Pecchioni, E.; Santo, A.P.; Ciaramitaro, V.C.; Saladino, M.L. Looking for the original materials and evidence of restoration at the Vault of the San Panfilo Church in Tornimparte (AQ). *Appl. Sci.* **2023**, *13*, 6492. [[CrossRef](#)]
43. Andreotti, A.; Izzo, F.C.; Bonaduce, I. Archaeometric study of the mural paintings by Saturnino Gatti and workshop in the Church of San Panfilo—Tornimparte (AQ). The study of organic materials. *Appl. Sci.* **2023**, *13*, 7153. [[CrossRef](#)]
44. Centamore, E.; Dramis, F. Note Illustrative Della Carta Geologica d'Italia Alla Scala 1:50.000, Foglio 358-Pescorocchiano. *ISPRA-Serv. Geol. D'Italia* **2010**, 147.
45. Murat, Z. Wall Paintings through the Ages: The Medieval Period (Italy, Twelfth to Fifteenth Century). *Archaeol. Anthr. Sci.* **2021**, *13*, 191. [[CrossRef](#)]

**Disclaimer/Publisher's Note:** The statements, opinions and data contained in all publications are solely those of the individual author(s) and contributor(s) and not of MDPI and/or the editor(s). MDPI and/or the editor(s) disclaim responsibility for any injury to people or property resulting from any ideas, methods, instructions or products referred to in the content.